

Spiropyrans and spirooxazines

6. * The spectral and kinetic properties of 5-(4,5-diphenyl-1,3-oxazol-2-yl)-substituted spironaphthopyrans: an experimental and theoretical study

A. V. Chernyshev,^{a*} I. V. Dorogan,^a N. A. Voloshin,^b A. V. Metelitsa,^a and V. I. Minkin^a

^a*Institute of Physical and Organic Chemistry, Southern Federal University,
194/2 prosp. Stachki, 344090 Rostov on Don, Russian Federation.*

E-mail: anatoly@ipoc.rsu.ru

^b*Southern Research Center of the Russian Academy of Sciences,
41 ul. Chekhova, 344006 Rostov on Don, Russian Federation*

Fax: +7 (863 2) 43 4667. E-mail: photo@ipoc.rsu.ru

The spectral and kinetic properties of 5-(4,5-diphenyl-1,3-oxazol-2-yl)spiro[indoline-naphthopyran] derivatives were studied by experimental and theoretical methods. The additional long-wavelength maximum in the absorption spectra of compounds studied is due to the introduction of a diphenyloxazole fragment and corresponds to a $\pi-\pi^*$ electronic transition with a partial charge transfer character. Substituents have little effect on the kinetic parameters of the spironaphthopyrans studied.

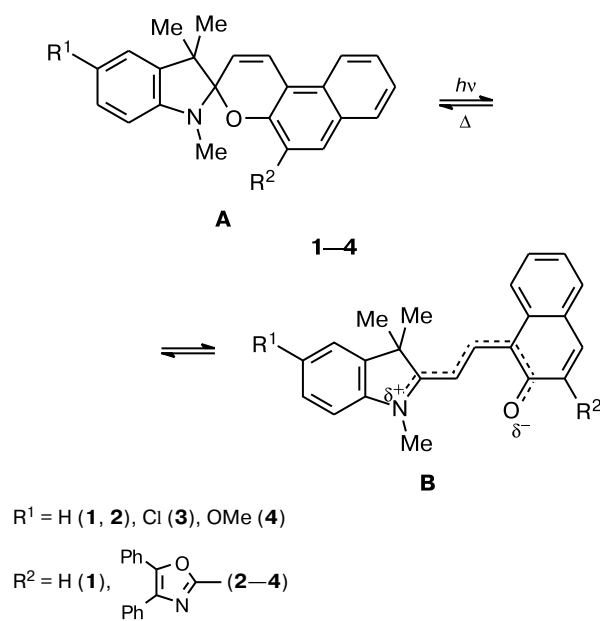
Key words: spiropyrans, photochromism, quantum chemical calculations, density functional theory, time-dependent density functional theory, PBE0 and B3LYP functionals.

The synthesis and investigations of new photochromic compounds to design polyfunctional materials for molecular electronics and chemical sensors is a key problem in modern chemistry. Among well-known classes of photochromic compounds, spiropyrans occupy a special position because they can vary their spectral and kinetic properties in a rather wide range depending on the molecular structure and can fairly easily be synthesized.^{2–4}

Photochromic transformations of spironaphthopyrans (SNPs) (Scheme 1) are due to thermally and photochemically reversible heterolytic dissociation of the C_{sp}–O bond in the cyclic isomer **A** followed by *cis*–*trans*-isomerization to the metastable merocyanine form **B**.^{2,3}

By introducing various functional fragments into spiropyran molecules one can obtain polyfunctional molecular systems that exhibit not only photochromic, but also photoswitchable magnetic,⁵ complex-forming,^{6–9} and fluorescence^{9–12} properties. Earlier,¹³ we have reported the synthesis of a photochromic 5-(4,5-diphenyl-1,3-oxazol-2-yl)substituted spiro[indoline-naphthopyran] whose merocyanine form is involved in reversible complexation with divalent heavy metal cations owing to participation of donor atoms of the 4,5-diphenyl-1,3-oxazole fragment in ion coordination. It was established that this fragment in the SNP structure is responsible for the appearance of an

Scheme 1



additional long-wavelength band in the absorption spectrum. However, no detailed studies to elucidate the nature of electronic transitions determining the spectral properties of such compounds were carried out. In addition, it is

* For Part 5, see Ref. 1.

interesting to investigate how the additional substituent in the indoline fragment of the molecule influences the spectral and kinetic properties of SNPs.

Experimental

Compounds **1–4** were synthesized according to the known procedures.^{13,14} Solutions were prepared using toluene and acetone (Aldrich, both of "spectroscopic" grade) as solvents.

Electronic absorption spectra and the kinetics of thermal recyclization of compounds **1–4** were recorded on an Agilent 8453 spectrophotometer equipped with a thermostating accessory. Solutions were irradiated with a filtered light from a high-pressure mercury lamp on a Newport 66902 equipment. Monochromatic radiation was cut with interference filters ($\lambda = 365$ nm). The optical radiation power was measured by a Newport Power Meter 2903-C photoreceiver.

Calculation Procedure

Geometry optimization for the systems corresponding to the stationary points on the ground-state potential energy surfaces (PESs) of the systems under study was performed within the framework of the density functional theory (DFT) using the PBE0 hybrid functional¹⁵ and the 6-311G* basis set. The search for transition states was done by the synchronous transit method (QST3). The nature of the stationary points was determined based on the results of vibrational frequency calculations (force constant matrix). The solvent effect was included within the framework of the CPCM model.¹⁶ The dielectric constant of the medium was set equal to that of acetone ($\epsilon = 20.7$).

The optimized geometric parameters of the structures corresponding to minima on the PES were used in the time-dependent DFT calculations of absorption spectra in acetone by the

TD PBE0/6-311G* and TD B3LYP/6-311G**//PBE0/6-311G* methods.

The energies of the first singlet electronic transitions of merocyanines were corrected using a linear dependence¹⁷

$$\Delta E_{\text{corr}} = -0.0963 + 0.9321\Delta E_{\text{calc}},$$

where ΔE_{calc} is the energy of the first singlet transition of merocyanine obtained from TD B3LYP/6-311G* calculations for a solution in ethanol ($\epsilon = 24.55$). Making use of this correlation in the TD B3LYP/6-311G**//PBE0/6-311G* calculations for a solution in acetone seems to be quite correct because the dielectric constants of acetone and ethanol are close and the geometric parameters of the systems in question computed using the PBE0 and B3LYP functionals^{18–20} and the same basis set differ insignificantly.

All calculations were carried out using the GAUSSIAN-03 program.²¹

Results and Discussion

Spectral properties. In the solutions in toluene and acetone, the proportion of the cyclic SNP isomers **A** (see Scheme 1) is almost 100%, as indicated by the lack of noticeable absorption in the visible region characteristic of the acyclic merocyanine structures **B**.^{2,3} The cyclic form **1** in toluene is characterized by a structured absorption band with maxima at 348 and 361 nm ($\epsilon = 4710$ and 4360 L mol⁻¹ cm⁻¹, respectively). The absorption bands of 5-diphenyloxazole-substituted compounds **2–4** have maxima at about 340 nm; however, the heterocyclic substituents cause the appearance of an additional long-wavelength band in the region 370–400 nm (Table 1). On going from toluene to acetone, the absorption bands un-

Table 1. Spectral properties of SNPs **1–4*** in solutions in toluene and acetone

SNP	Isomer	Toluene					Acetone		
		$\lambda_{\text{max}}^{\text{abs}}$ ($\epsilon \cdot 10^3/\text{L mol}^{-1} \text{cm}^{-1}$)	$(\lambda_{\text{max}}^{\text{ex}})^{\text{flu}}$	$\lambda_{\text{max}}^{\text{flu}}$	$(\lambda_{\text{max}}^{\text{ex}})^{\text{ph}}$	$\lambda_{\text{max}}^{\text{ph}}$	$\lambda_{\text{max}}^{\text{abs}}$ ($\epsilon \cdot 10^3/\text{L mol}^{-1} \text{cm}^{-1}$)	$(\lambda_{\text{max}}^{\text{ex}})^{\text{flu}}$	$\lambda_{\text{max}}^{\text{flu}}$
1	A	300 (9.52), 313 (7.79), 348 (4.71), 361 (4.36)	—	—	—	—	346 (4.20), 359 (4.00)	—	—
	B	562	558	600	—	—	562	560	600
2	A	304 (25.62), 342 (19.66), 380** (8.30), 395** (5.90)	398, 404	420, 432**	396	574, 625, 680**	338 (19.10), 375 (6.30), 392 (4.60)	380	410
	B	596	590	618	—	—	588	580	620
3	A	306 (30.67), 342 (23.13), 380 (8.63), 396 (6.12)	385, 393	410, 430, 450**	385, 393	580, 630, 685**	337 (21.90), 380 (6.38), 400 (3.84)	381, 400	426
	B	—	—	—	—	—	595	590	625
4	A	309 (33.70), 341 (24.40), 380 (9.40), 397 (6.50)	385, 400	410**, 430, 465	370, 400	577, 630, 690	334 (21.28), 378** (6.77), 394 (5.02)	398, 408	432, 463**
	B	—	—	—	—	—	602	590	630

* Absorption at 293 K, luminescence at 77 K (glass-forming mixture toluene—ethanol—Et₂O); $\lambda_{\text{max}}^{\text{abs}}$, $(\lambda_{\text{max}}^{\text{ex}})^{\text{flu}}$, $\lambda_{\text{max}}^{\text{flu}}$, $(\lambda_{\text{max}}^{\text{ex}})^{\text{ph}}$ and $\lambda_{\text{max}}^{\text{ph}}$ (nm) are the wavelengths of maxima in the absorption spectrum, fluorescence excitation spectrum, fluorescence spectrum, phosphorescence excitation spectrum, and phosphorescence spectrum, respectively.

** Shoulder.

dergo a small hypsochromic shift. The fluorescence maxima of spirocyclic isomers lie at 420–430 nm. As the solution temperature decreases to 77 K, the fluorescence intensity considerably increases and phosphorescence characterized by a structured band with maxima at 580 and 630 nm appears. Unlike compounds **2A**–**4A**, the unsubstituted SNP **1A** emits no luminescence (see Table 1).

At room temperature, the compounds under study exhibit no photochromism. A decrease in temperature of SNP solutions allows one to disclose their photochromic properties, which are not observed under steady-state irradiation at 293 K owing to high rate of the reverse thermal recyclization **B** → **A**. UV irradiation of colorless SNP solutions at $T < 273$ K is followed by their coloration. In the electronic absorption spectra, this is accompanied by the appearance of long-wavelength absorption bands with maxima in the region 562–602 nm (see Table 1, Fig. 1). This absorption is characteristic of the acyclic merocyanine structures **B**.^{2,3}

The introduction of a diphenyloxazolyl substituent (SNPs **2**–**4**) causes a bathochromic shift of absorption maxima of the merocyanine forms **B** (see Table 1) relative

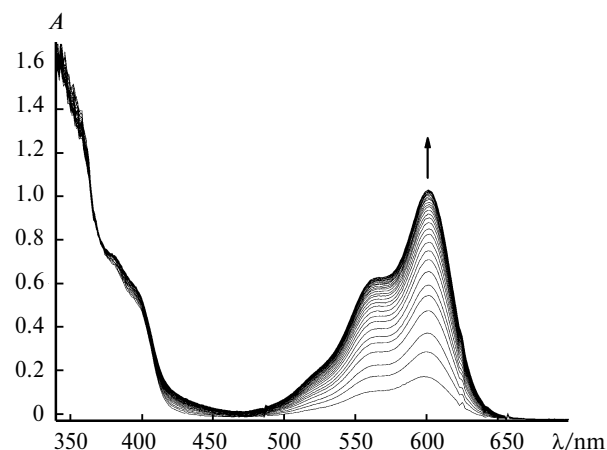


Fig. 1. Absorption spectra of compound **3** in acetone obtained upon irradiation at $\lambda = 365$ nm; the spectra were acquired with 2 s intervals, $C(\mathbf{3}) = 9.5 \cdot 10^{-5}$ mol L⁻¹, $T = 259$ K.

to the bands in the spectrum of unsubstituted SNP **1**. The merocyanine forms **B** of the SNPs **1**–**4** emit bright fluorescence in the region 550–720 nm; maxima of the fluorescence

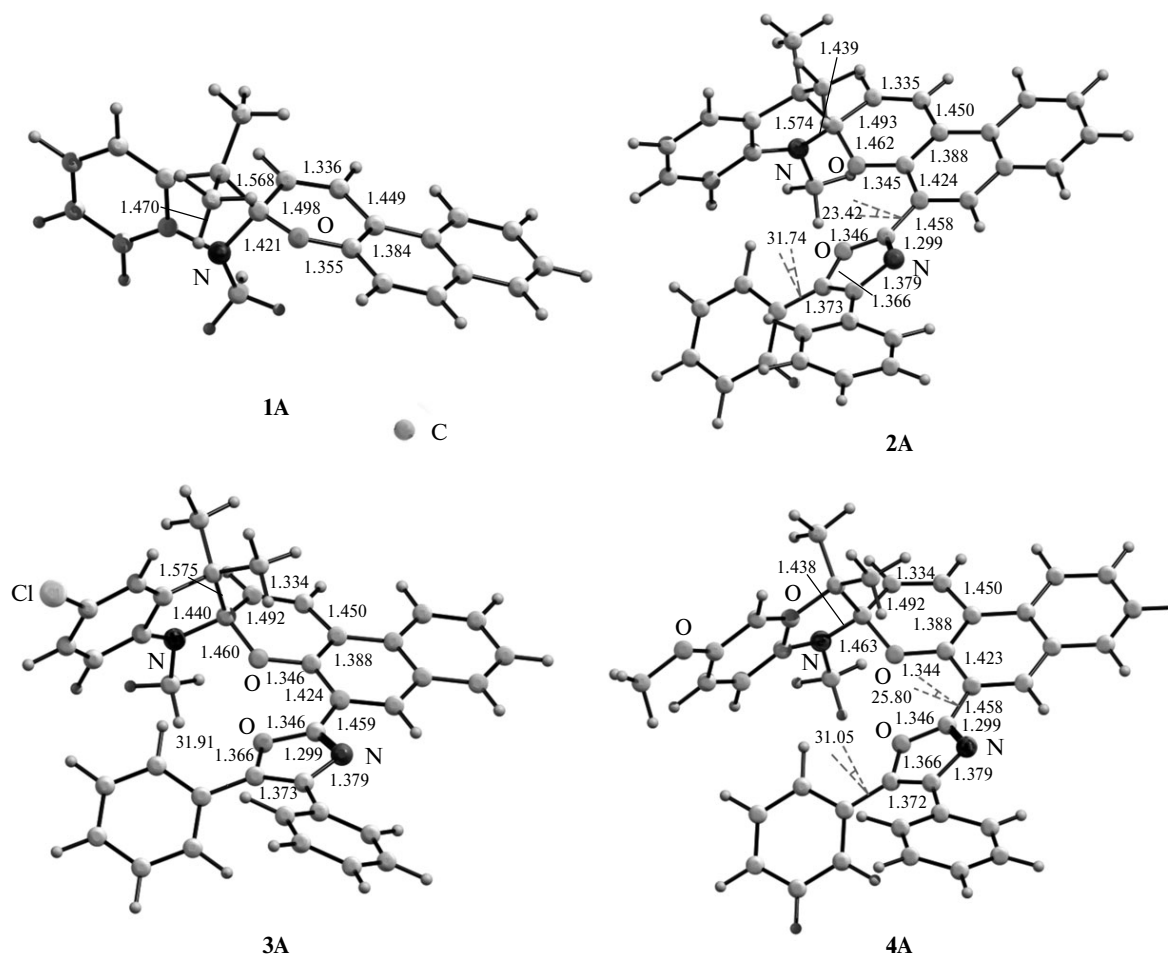


Fig. 2. Geometric parameters of spironaphthopyrans **1A**–**4A** in solution in acetone obtained from PBE0/6-311G* calculations. Here and in Figs 3 and 8 shown are the bond lengths (Å) and dihedral angles (deg).

bands of the isomers **2B–4B** undergo a bathochromic shift relative to the spectrum of compound **1B** (see Table 1).

To elucidate the nature of the electronic transitions responsible for maxima in the absorption spectra of SNPs and their open forms, we calculated the excitation energies within the framework of the TD DFT approach. The results obtained are listed in Tables 2 and 3.

The calculated structures of the cyclic and open SNP isomers are presented in Figs 2 and 3.

From the results of calculations it follows that the absorption spectra of the compounds under study strongly depend on the substituents in the indoline and naphthopyran fragments. In particular, for the unsubstituted SNP the strongest absorption band corresponds to the $\pi-\pi^*$ -transition $S_0 \rightarrow S_2$ (major contribution from HOMO-1 \rightarrow LUMO) localized on the naphthopyran fragment. The first singlet transition corresponds to a weak band (HOMO \rightarrow LUMO) characterizing charge transfer from the indoline to the naphthopyran fragment.

The introduction of the diphenyloxazolyl substituent into the naphthopyran fragment causes the appearance of an additional maximum on the long-wavelength absorption band. Strong second and third singlet transitions (HOMO-2 \rightarrow LUMO and HOMO-1 \rightarrow LUMO, respec-

Table 2. Excitation energies E_{calc} (eV) and oscillator strengths f of the first four singlet transitions of the spirocyclic forms of the spironaphthopyran derivatives **1A–4A** in solution in acetone: results of TD PBE0/6-311G** calculations and experimental values

SNP	Transition	TD PBE0/6-311G* calculations		Experi- ment,
		f	E_{calc}	E_{obs}
1A	$S_0 \rightarrow S_1$	0.092	3.490	3.454
	$S_0 \rightarrow S_2$	0.154	3.746	3.584
	$S_0 \rightarrow S_3$	0.021	4.337	—
	$S_0 \rightarrow S_4$	0.036	4.565	—
2A	$S_0 \rightarrow S_1$	0.018	3.333	3.163
	$S_0 \rightarrow S_2$	0.125	3.364	3.307
	$S_0 \rightarrow S_3$	0.483	3.486	3.669
	$S_0 \rightarrow S_4$	0.020	3.890	—
3A	$S_0 \rightarrow S_1$	0.131	3.369	3.100
	$S_0 \rightarrow S_2$	0.021	3.409	3.263
	$S_0 \rightarrow S_3$	0.472	3.478	3.473
	$S_0 \rightarrow S_4$	0.173	3.900	3.680
4A	$S_0 \rightarrow S_1$	0.004	3.029	3.147
	$S_0 \rightarrow S_2$	0.130	3.366	3.280
	$S_0 \rightarrow S_3$	0.485	3.500	3.473
	$S_0 \rightarrow S_4$	0.006	3.567	3.713

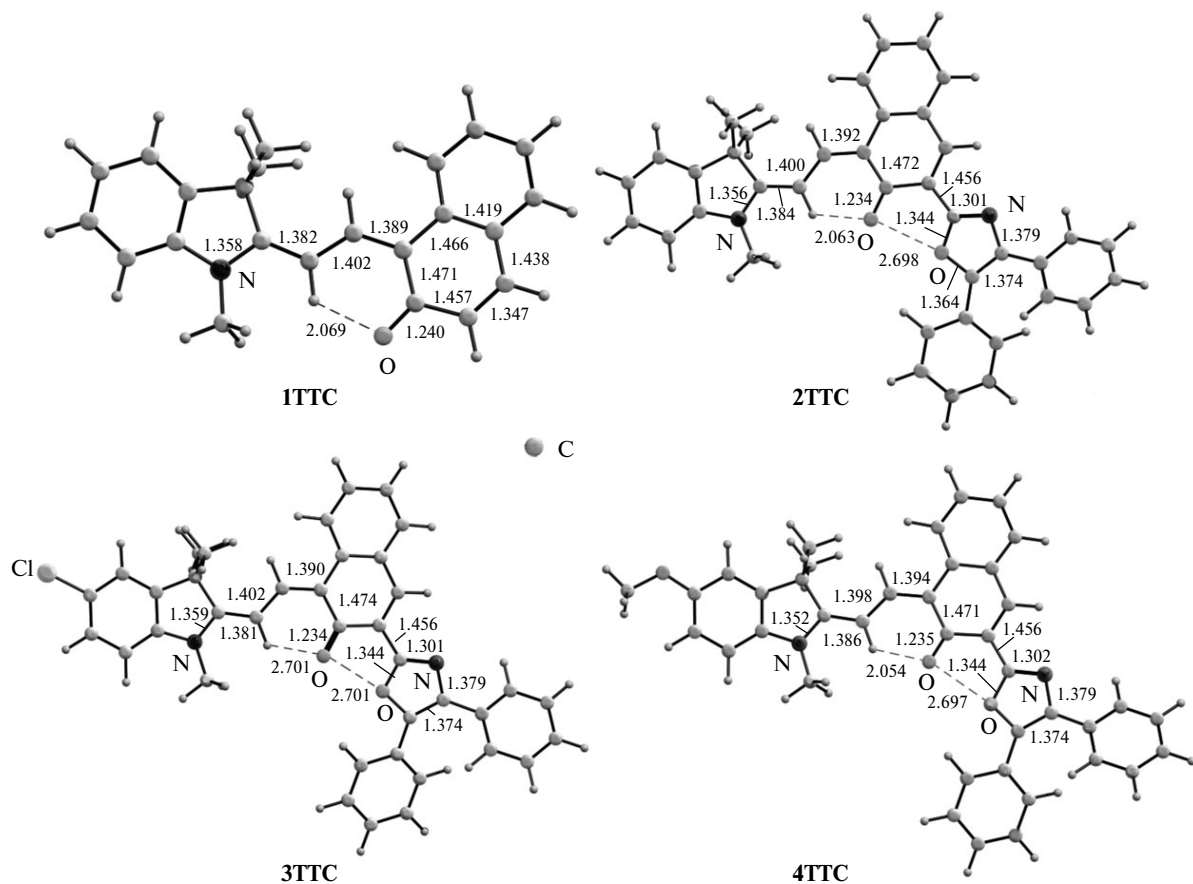


Fig. 3. Geometric parameters of the merocyanine forms **1TTC**, **2TTC**, **3TTC**, and **4TTC** in solution in acetone obtained from PBE0/6-311G* calculations.

Table 3. Excitation energies E_{calc} (eV) and oscillator strengths f of the first four singlet transitions of the merocyanines **1TTC**–**4TTC*** in solution in acetone calculated by the TD PBE0/6-311G** and TD B3LYP/6-311G**//PBE0/6-311G* methods, excitation energies of the first singlet transitions obtained from TD B3LYP/6-311G**//PBE0/6-311G* calculations with inclusion of linear correction E_{corr} (eV), and the observed excitation energies E_{obs} (eV)

SNP	Transition	Calculations					Experiment, E_{obs}
		TD PBE0/6-311G*		TD B3LYP/6-311G**//PBE0/6-311G*			
		f	E_{calc}	f	E_{calc}	E_{corr}	
1TTC	$S_0 \rightarrow S_1$	0.936	2.660	0.908	2.610	2.336	2.206
	$S_0 \rightarrow S_2$	0	3.002	0	2.905		
	$S_0 \rightarrow S_3$	0.101	3.446	0.090	3.311		
	$S_0 \rightarrow S_4$	0.132	3.918	0.114	3.799		
2TTC	$S_0 \rightarrow S_1$	0.787	2.474	0.682	2.402	2.142	2.109
	$S_0 \rightarrow S_2$	0.286	2.820	0.318	2.684		
	$S_0 \rightarrow S_3$	0.002	3.003	0.002	2.889		
	$S_0 \rightarrow S_4$	0.306	3.424	0.283	3.290		
3TTC	$S_0 \rightarrow S_1$	0.805	2.461	0.674	2.384	2.125	2.084
	$S_0 \rightarrow S_2$	0.322	2.779	0.383	2.648		
	$S_0 \rightarrow S_3$	0.003	2.992	0.003	2.880		
	$S_0 \rightarrow S_4$	0.316	3.446	0.288	3.312		
4TTC	$S_0 \rightarrow S_1$	0.908	2.425	0.836	2.359	2.102	2.060
	$S_0 \rightarrow S_2$	0.2432	2.827	0.238	2.684		
	$S_0 \rightarrow S_3$	0.003	3.014	0.002	2.898		
	$S_0 \rightarrow S_4$	0.268	3.349	0.256	3.210		

* **TTC** is the *trans-trans-cis*-isomer.

tively) are of $\pi-\pi^*$ character with partial redistribution of the electron density from the phenyl rings of the substituent to the naphthopyran fragment (Fig. 4). In this case, the first singlet transition ($\text{HOMO} \rightarrow \text{LUMO}$) is of the same character as for the unsubstituted compound. In addition to these changes, the absorption bands of the diphenyloxazolyl derivatives undergo a bathochromic shift compared to the spectrum of the unsubstituted compound; this agrees with the experimental data.

An additional electron-withdrawing substituent (Cl) in the indoline fragment of molecule **3A** is responsible for

a significant decrease in the intensity of the second singlet transition ($\text{HOMO}-1 \rightarrow \text{LUMO}$). This is due to inversion of the HOMO and HOMO-1 states of compound **3A** compared to the unsubstituted structure **2A**. The shape of the HOMO for **3A** almost matches that of the HOMO-1 for **2A**. Thus, the strongest long-wavelength bands correspond to the transitions $S_0 \rightarrow S_1$ ($\text{HOMO}-2 \rightarrow \text{LUMO}$) and $S_0 \rightarrow S_3$ ($\text{HOMO} \rightarrow \text{LUMO}$).

An additional electron-donating substituent OMe introduced into the indoline fragment of molecule **4A** influences the spectrum oppositely. By and large, the nature of

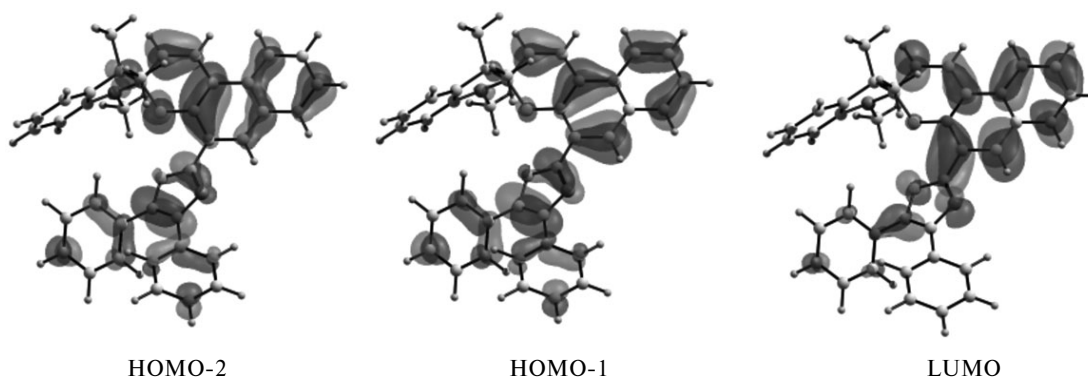


Fig. 4. Molecular orbitals of compound **2A** responsible for the transitions $S_0 \rightarrow S_2$ and $S_0 \rightarrow S_3$. Hereafter, the MO contours are plotted at a level of 0.03 au.

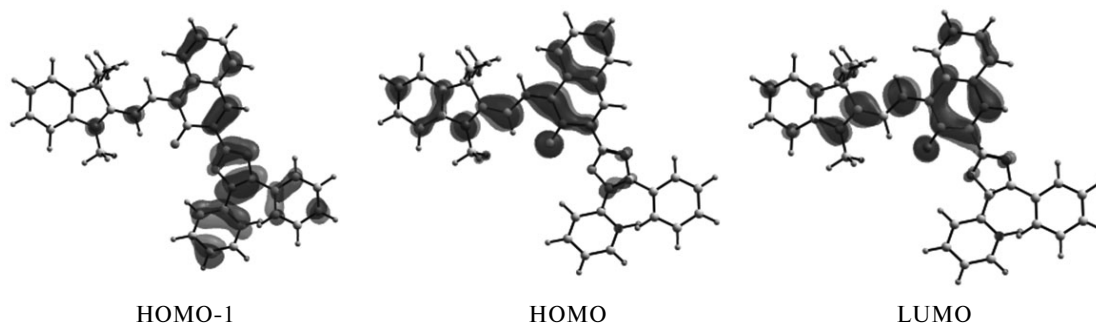


Fig. 5. Molecular orbitals of compound **2B** responsible for the transitions $S_0 \rightarrow S_1$ and $S_0 \rightarrow S_2$.

transitions remains the same as for the unsubstituted molecule **2A**. Only a bathochromic shift of absorption maxima is observed, the largest shift (by about 0.3 eV) being observed for the absorption band corresponding to the weak first singlet transition (HOMO \rightarrow LUMO) characterizing charge transfer from the indoline fragment to the spiro-conjugated molecular fragment.

The differences between the calculated and experimentally determined energies of the singlet transitions in the SNPs under study lie in the range 0.005–0.27 eV, being on the average at most 0.2 eV.

If for the SNPs both long-wavelength absorption bands correspond to the $\pi-\pi^*$ transitions due to redistribution of the electron density in the chromene fragment (including the diphenyloxazolyl substituent), for the corresponding merocyanine isomers these bands are due to electronic transitions of essentially different nature. The strongest transition $S_0 \rightarrow S_1$ (HOMO \rightarrow LUMO) is of $\pi-\pi^*$ character not related to the changes in the electron density on the diphenyloxazolyl substituent, whereas the second singlet transition (HOMO-1 \rightarrow LUMO) is of clearly defined charge-transfer character. By and large, the electron den-

sity is redistributed from the diphenyloxazolyl substituent to other molecular fragments (Fig. 5).

Substituents in the indoline moieties of the merocyanines affect only positions of the long-wavelength absorption maxima and do not influence the nature of the corresponding electronic transitions. The introduction of the electron-withdrawing substituent (Cl) causes a bathochromic shift of these absorption bands. The electron-donating substituent (OMe) makes this effect more pronounced. The calculated changes in the spectroscopic properties of the compounds under study are in qualitative agreement with experimental observations. An additional linear correction of position of the long-wavelength absorption maxima of the merocyanines significantly reduces computational errors (see Table 3).

Kinetic properties. We analyzed the dependence of the rate constants for the thermal reaction $\mathbf{B} \rightarrow \mathbf{A}$ on the solution temperature. From the data shown in Fig. 6 it follows that the temperature dependences of the rate constants $k_{\mathbf{B}\mathbf{A}}$ for the thermal reactions in acetone are of the Arrhenius type (Fig. 7). This allowed the activation energies of the thermal bleaching reactions to be determined (Table 4).

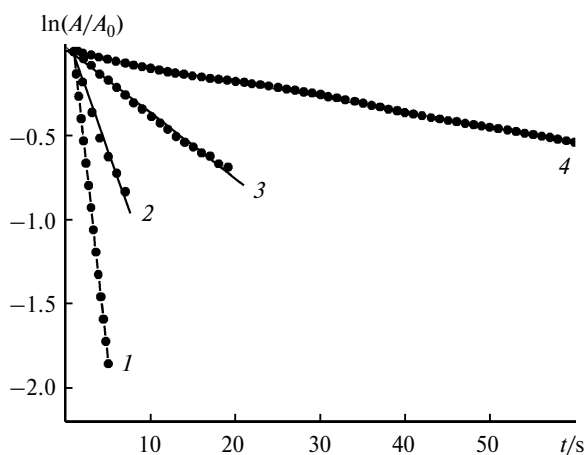


Fig. 6. Linear anamorphoses of the kinetic curves of thermal bleaching of irradiated solution of SNP **3** in acetone at $T=274$ (**1**), 266 (**2**), 259 (**3**), and 250 K (**4**).

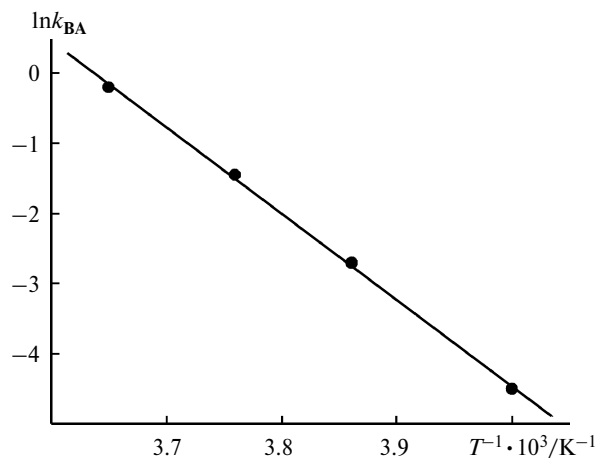


Fig. 7. Logarithm of the rate constant for the reverse ($\mathbf{B} \rightarrow \mathbf{A}$) thermal reaction of SNP **3** plotted vs. temperature (with acetone as solvent).

Table 4. Rate constants ($T = 293$ K) for, and activation energies of, the reverse thermal reaction of isomerization $\mathbf{B} \rightarrow \mathbf{A}$ of SNPs in acetone

SNP	$k_{\text{BA}}/\text{s}^{-1}$	$E_{\text{a}}^{\text{BA}}/\text{kcal mol}^{-1}$
1	29.019	18.9
2	11.144	20.9
3	8.147	16.6
4	4.143	24.9

The mechanism of spirocyclization of the merocyanine forms of indoline spiropyrans was studied in detail (see, *e.g.*, Ref. 22). It was assumed that the initial reactant is the thermodynamically most stable merocyanine isomer (in this case, the *trans-trans-cis*-isomer, or the TTC-isomer). Computer simulation of thermal relaxation of the merocyanine forms of indoline spiropyrans suggested that the limiting stage of the reaction is rotation of one molec-

ular fragment about the central C—C bond in the methine bridge. This may result in either a kinetically unstable *cis*-intermediate undergoing a low-barrier transformation to a closed form or (if the formation of such an intermediate is sterically hindered) the cyclic form itself. In all cases, the kinetic properties of the reverse reaction can be evaluated by estimating the activation barrier to the *cis*—*trans*-isomerization of merocyanine. The calculated geometric parameters of the corresponding transition states are shown in Fig. 8.

According to calculations, for all compounds investigated the closed forms are thermodynamically more stable than the corresponding merocyanine isomers. The introduction of the diphenyloxazolyl substituent into the naphthopyran fragment slightly destabilizes the open form. An additional electron-withdrawing substituent (Cl) in the indoline moieties of the compounds studied enhances this effect, whereas the electron-donating substituent (OMe) cause it to weaken (Table 5).

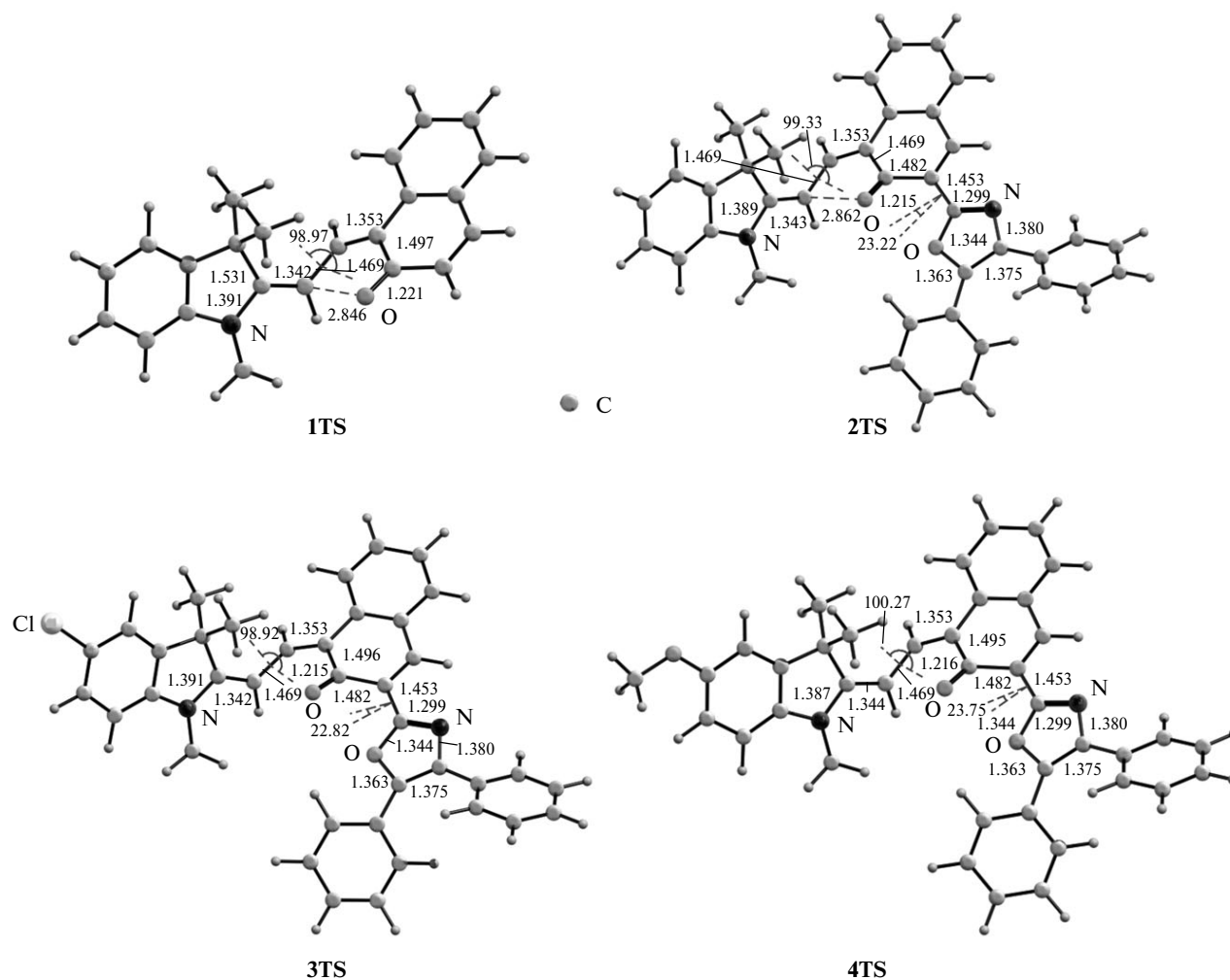


Fig. 8. Geometric parameters of transition states (TS) of the reverse thermal reaction 1TS, 2TS, 3TS, and 4TS in solution in acetone obtained from PBE0/6-311G* calculations.

Table 5. Total energies calculated taking account of zero-point vibrational energy correction $E_{\text{tot}} + \text{ZPE}$ (au) and the relative energies ΔE (kcal mol⁻¹) of the structures corresponding to the critical points on the reaction pathways of thermal relaxation of the merocyanine **TTC**-isomers of spironaphthopyrans **1–4**, and the imaginary vibrational frequencies ν_{im} (cm⁻¹) of the structures of transition states (**TS**) in the solution in acetone obtained from PBE0/6-311G** calculations

Structure	$-(E_{\text{tot}} + \text{ZPE})$	ν_{im}	ΔE
1A	1017.702657	—	0
1TS	1017.671032	i202.6	19.8
1TTC	1017.698675	—	2.5
2A	1723.838754	—	0
2TS	1723.803932	i179.1	21.9
2TTC	1723.832228	—	4.1
3A	2183.312774	—	0
3TS	2183.304650	i158.0	21.9
3TTC	2183.277887	—	5.1
4A	1838.229602	—	0
4TS	1838.194650	i205.8	21.9
4TTC	1838.224420	—	3.3

In all cases, the activation barriers to reactions were estimated from the total energy differences between the **TTC**-isomer and the corresponding transition state calculated with inclusion of zero-point vibrational energies. The calculated activation barriers to the reverse thermal reaction for the merocyanines **1TTC** (17.3), **2TTC** (17.8), and **3TTC** (16.8 kcal mol⁻¹) are in good agreement with experimental data (18.9, 20.9 and 16.6 kcal mol⁻¹, respectively). For the merocyanine **3TTC** with methoxy group in the indoline fragment, the calculated and experimental activation barriers (18.7 and 24.9 kcal mol⁻¹, respectively) differ to a greater extent.

Summing up, based on the experimental data and results of quantum chemical calculations, we established that the additional long-wavelength maximum in the absorption spectra of 5-(4,5-diphenyl-1,3-oxazol-2-yl)spiro[indolyl-naphthopyran] derivatives appeared upon introduction of the diphenyloxazolyl substituent into the naphthopyran fragment and corresponding (for the cyclic form) to the singlet $\pi-\pi^*$ -transition with partial charge transfer from the diphenyloxazolyl substituent, is of well-defined charge transfer character for the open form. Electron-donating and electron-withdrawing substituents in the indoline fragments of the merocyanines are responsible for bathochromic shifts of the long-wavelength maxima in the absorption spectra without changing the nature of the corresponding electronic transitions.

The kinetic parameters of the SNP transitions under study depend only slightly on substituents. The introduction of the diphenyloxazolyl substituent into the naphthopyran fragment results in insignificant destabilization of

the open form and an increase in the activation barrier to the reverse thermal reaction. Additional electron-withdrawing substituent (Cl) in the indoline fragments of the molecules in question causes this barrier to decrease, whereas the electron-donating substituent (OMe) leads to its decrease.

This work was financially supported by the Ministry of Education and Science of the Russian Federation (Federal Target Program "Scientific and Pedagogical Staff of Innovation Russia, Years 2009–2013", under the State Contract No. P2346) and the Russian Foundation for Basic Research (Project No. 09-03-93115).

References

- N. A. Voloshin, E. B. Gaeva, A. V. Chernyshev, A. V. Metelitsa, V. I. Minkin, *Izv. Akad. Nauk, Ser. Khim.*, 2009, **58**, 156 [*Russ. Chem. Bull., Int. Ed.*, 2009, **58**, 156].
- R. C. Bertelson, in *Organic Photochromic and Thermochromic Compounds. Topics in Applied Chemistry*, Eds J. C. Crano, R. J. Guglielmetti, Plenum Press, New York, 1999, Vol. **1**, p. 11.
- V. I. Minkin, *Chem. Rev.*, 2004, **104**, 2751.
- B. S. Luk'yanov, M. B. Luk'yanova, *Khim. Geterotsykl. Soedin.*, 2005, 321 [*Chem. Heterocycl. Compd. (Engl. Transl.)*, 2005, No. 3].
- S. M. Aldoshin, *J. Photochem. Photobiol. A: Chem.*, 2008, **200**, 19.
- M. Inouye, *Coord. Chem. Rev.*, 1996, **148**, 265.
- M. V. Alfimov, O. A. Fedorova, S. P. Gromov, *J. Photochem. Photobiol. A: Chem.*, 2003, **158**, 183.
- S. Kum, H. Nishihara, *Struct. Bond*, 2007, **123**, 79.
- S. A. Ahmed, M. Tanaka, H. Ando, K. Tawa, K. Kimura, *Tetrahedron*, 2004, **60**, 6029.
- J.-R. Chen, J.-B. Wong, P.-Y. Kuo, D.-Y. Yang, *Org. Lett.*, 2008, **10**, 4823.
- M. Tomasulo, E. Deniz, R. J. Alvarado, F. M. Raymo, *J. Phys. Chem. C*, 2008, **112**, 8038.
- B. Seefeldt, R. Kasper, M. Beining, J. Mattay, J. Arden-Jacob, N. Kemnitzer, K. H. Drexhage, M. Heilemann, M. Sauer, *Photochem. Photobiol. Sci.*, 2010, **9**, 213.
- A. V. Chernyshev, N. A. Voloshin, I. M. Raskita, A. V. Metelitsa, V. I. Minkin, *J. Photochem. Photobiol. A: Chem.*, 2006, **184**, 289.
- N. A. Voloshin, A. V. Chernyshev, A. V. Metelitsa, V. I. Minkin, *Khim. Geterotsykl. Soedin.*, 2011, No. 4 [*Chem. Heterocycl. Compd. (Engl. Transl.)*, 2011, No. 4].
- J. P. Perdew, K. Burke, M. Ernzerhof, *Phys. Rev. Lett.*, 1996, **77**, 3865.
- V. Barone, M. Cossi, *J. Phys. Chem. A*, 1998, **102**, 1995.
- M. Guillaume, B. Champagne, F. Zutterman, *J. Phys. Chem. A*, 2006, **110**, 13007.
- A. D. Becke, *Phys. Rev. A*, 1991, **91**, 651.
- A. D. Becke, *J. Chem. Phys.*, 1993, **98**, 5648.
- C. Lee, W. Yang, R. G. Parr, *Phys. Rev. B*, 1988, **37**, 785.
- M. J. Frisch, G. W. Trucks, H. B. Schlegel, G. E. Scuseria, M. A. Robb, J. R. Cheeseman, J. A. Montgomery, Jr., T. Vreven, K. N. Kudin, J. C. Burant, J. M. Millam, S. S.

Iyengar, J. Tomasi, V. Barone, B. Mennucci, M. Cossi, G. Scalmani, N. Rega, G. A. Petersson, H. Nakatsuji, M. Hada, M. Ehara, K. Toyota, R. Fukuda, J. Hasegawa, M. Ishida, T. Nakajima, Y. Honda, O. Kita, H. Nakai, M. Klene, X. Li, J. E. Knox, H. P. Hratchian, J. B. Cro, C. Adamo, J. Jaramillo, R. Gomperts, R. E. Stratmann, O. Yazyev, A. J. Austin, R. Cammi, C. Pomelli, J. W. Ochterski, P. Y. Ayala, K. Morokuma, G. A. Voth, P. Salvador, J. J. Dannenberg, V. G. Zakrzewski, S. Dapprich, A. D. Daniels, M. C. Strain, O. Farkas, D. K. Malick, A. D. Rabuck, K. Raghavachari, J. B. Foresman, J. V. Ortiz, Q. Cui, A. G. Baboul, S. Clifford, J. Cioslowski, B. B. Stefanov, G. Liu, A. Liashenko,

P. Piskorz, I. Komaromi, R. L. Martin, D. J. Fox, T. Keith, M. A. Al. Laham, C. Y. Peng, A. Nanayakkara, M. Challacombe, P. M. W. Gill, B. Johnson, W. Chen, M. W. Wong, C. Gonzalez, J. A. Pople, *Gaussian 03*, Revision C.02, Gaussian, Inc., Wallingford (CT), 2004.
22. Y. Sheng, J. Leszynski, A. A. Garcia, R. Rosario, D. Gust, J. Springer, *J. Phys. Chem. B*, 2004, **108**, 16233.

*Received September 23, 2010;
in revised form December 7, 2010*